



HAL
open science

Silicon etching in a pulsed HBr/O₂ plasma. II. Pattern transfer

Moritz Haass, M. Darnon, Gilles Cunge, Olivier Joubert

► **To cite this version:**

Moritz Haass, M. Darnon, Gilles Cunge, Olivier Joubert. Silicon etching in a pulsed HBr/O₂ plasma. II. Pattern transfer. *Journal of Vacuum Science & Technology B Microelectronics and Nanometer Structures*, 2015, 12 (118), 10.1116/1.4917231 . hal-01878012

HAL Id: hal-01878012

<https://hal.univ-grenoble-alpes.fr/hal-01878012>

Submitted on 6 Apr 2020

HAL is a multi-disciplinary open access archive for the deposit and dissemination of scientific research documents, whether they are published or not. The documents may come from teaching and research institutions in France or abroad, or from public or private research centers.

L'archive ouverte pluridisciplinaire **HAL**, est destinée au dépôt et à la diffusion de documents scientifiques de niveau recherche, publiés ou non, émanant des établissements d'enseignement et de recherche français ou étrangers, des laboratoires publics ou privés.



Distributed under a Creative Commons Attribution 4.0 International License

Silicon etching in a pulsed HBr/O₂ plasma. II. Pattern transfer

Moritz Haass, Maxime Darnon,^{a)} Gilles Cunge, and Olivier Joubert

LTM (CNRS/UJF-Grenoble1/CEA), 17 Avenue des Martyrs, 38054 Grenoble Cedex 9, France

(Received 29 September 2014; accepted 17 March 2015; published 9 April 2015)

The strong impact of synchronized plasma pulsing on an HBr/O₂ silicon pattern etch process is studied with respect to the continuous process. This article focuses on blanket etch rates and a detailed analysis of the etched profiles, where several significant features of plasma pulsing are identified. First, the time compensated (TC) silicon etch rate is increased while the SiO₂ TC etch rate is decreased at a low duty cycle, whereby the selectivity between silicon and SiO₂ etching is strongly increased. Furthermore, the thickness of the sidewall passivation layer is reduced, thereby guiding the etched profile. Finally, the overall homogeneity is increased compared to the continuous wave etching process. © 2015 American Vacuum Society.

[<http://dx.doi.org/10.1116/1.4917231>]

I. INTRODUCTION

Plasmas composed of HBr/O₂ are often used for silicon etch processes such as gate etch processes or shallow trench isolation etching and, because silicon etching in such chemistries is rather well understood, it is a perfect candidate to study the impact of plasma pulsing upon the gas phase and the plasma–surface interaction. The goal is to understand the fundamental differences between a continuous and a pulsed plasma, and how the changes in plasma creation affect the resulting pattern transfer. In Paper I, we have demonstrated the strong impact of plasma pulsing upon the ion flux and ion energy.¹ It was shown that especially the duty cycle (dc) and not the pulse frequency has a significant impact upon these parameters.

In this article, we focus on the influence of plasma pulsing upon the etch mechanisms and the pattern transfer in the HBr/O₂ plasma. Previous experiments have already shown the reduction of plasma-induced damage in pulsed plasmas,^{2–4} often by using scanning electron microscope (SEM) imaging, ellipsometric measurements, and x-ray photoelectron spectroscopy (XPS) topographic analysis of the sidewall passivation layers (SPLs).

Many authors have investigated the etch mechanisms in HBr/O₂ plasmas for silicon and SiO₂.^{5–13} The fundamental mechanisms for Si and SiO₂ etching are summarized in the following, wherein a very small percentage of oxygen in the feed gas stock is considered. Bromine-, hydrogen-, and, to a minor extent, also oxygen-containing ions hit the silicon surface, dissociate, destroy bonds, and form a halogen-rich amorphous layer, also called a reactive etch layer (REL), with incorporated H, Br, and some O atoms. Depending upon the ion energy, the pressure and the feed gas stock flow levels, the amorphous layer can vary in thickness and composition. Because H atoms are considerably smaller than the other particles, they may penetrate deeper into the silicon layer, whereupon Si atoms can desorb owing to collisional impact or can be incorporated into volatile species such as SiBr₄. Hydrogen-containing molecules such as SiH₂Br₂ are even more volatile,¹³ but the silicon etching is not

spontaneous in HBr/O₂ chemistries and a threshold ion energy of ~10 eV is needed¹³ to allow the etching to proceed. Because the Si–O bond is stronger than the Si–Br bond⁹ and oxygen-containing molecules are less volatile, the ion-enhanced chemical sputtering rate induced by the plasma can be decreased if oxygen atoms bind silicon to the layer. On the other hand, Br and H radicals from the gas phase adsorb on the surface of the amorphous layer and strongly increase the formation of volatile Si molecules.

In contrast to silicon etching, SiO₂ is etched very slowly. Because the formation of Si–O bonds is thermodynamically favored compared to Si–Br bonds, chemically enhanced etching of SiO₂ is minimized. Oxygen atoms are preferentially sputtered from the surface,^{11,14} leaving free spaces for Br to form Si–Br bonds and, subsequently, volatile molecules. On the other hand, oxygen atoms from the gas phase can spontaneously replace Br bonded to Si,^{5,10,11} strongly minimizing the formation of volatile products. If SiO₂ is used as an etch mask for silicon, silicon containing species with a high sticking coefficient, such as SiBr, can be deposited on the surface from the plasma gas phase. While this has a minimal effect upon the silicon etch, these products can bind strongly on dangling bonds of the SiO₂ surface, thereby decreasing the effective etch rate.¹⁰ Oxygen from the gas phase can further harden this deposited layer, so an increased oxygen flow and/or an increase of depositing species can slow down the SiO₂ etch rate.

In comparison, the silicon etching yield is strongly enhanced by a large surface coverage of Br radicals and the activation energy is rather low, while the SiO₂ etching needs quite a lot of activation energy even if the surface is fully covered with Br radicals.¹⁵ Therefore, it is likely that, in most process conditions, the etch rate for silicon is limited by the Br radical flux while the SiO₂ etch rate is limited by the ion energy and the ion flux.

II. EXPERIMENTAL SETUP

The experiments are carried out in a commercially available 300 mm AdvantEdge™ DPS etch tool from Applied Materials, Inc. The plasma is sustained by two inductively coupled plasma coils (source) powered at 13.56 MHz, while

^{a)}Electronic mail: Maxime.Damon@USherbrooke.ca

the chuck is biased via a capacitively coupled radio frequency power source (bias) also working at 13.56 MHz. The power supply is modified with the Pulsync™ system to allow pulsing of the source and bias power with frequencies between 100 Hz and 20 kHz and duty cycles between 10% and 90%. More details about the etch reactor can be found in the literature.¹⁶

In this article, a synchronously pulsed HBr/O₂ plasma at 20 mTorr with a gas flow of 200 (HBr) and 5 (O₂) sccm is investigated for silicon pattern etch applications. The source and bias power are set to 750 and 200 W, respectively.

Etch rates on blanket wafers are acquired by using an *ex-situ* small spot, multiangle, laser based, multiwavelength S300-Ultra ellipsometer from Rudolph Technologies. The measurements are performed at 25 locations distributed in circles whose centers are the middle of the 300 mm wafer, with one point taken from the center, 8 from a circle with radius 48.3 mm, and 16 from a circle with radius 96.7 mm. For SiO₂ etch rate measurement, 300 mm silicon wafers coated with 85 nm of SiO₂ were etched for 1 min of plasma on time. For Si etch rate measurements, 300 mm silicon wafers coated with 50 nm of SiO₂ and 280 nm of polysilicon were etched for 40 s of plasma on time.

Furthermore, cross section images of the etched microstructures are obtained with a commercially available JSM-7500F field emission scanning SEM from JEOL Ltd. In theory, the maximal resolution is 1.4 nm at an acceleration voltage of 1 kV, but in practice, the resolution is more likely to be around 3 nm. Finally, XPS measurements are realized with a customized Thermo Fisher Scientific Theta 300 spectrometer connected under vacuum to the wafer transfer system of the etch chamber, allowing the 300 mm wafers to be analyzed quasi *in-situ*.

Two sets of patterned wafers have been used in this study. In both cases, the etched stack consists in 300 mm p-type Czochralski silicon wafers coated with SiO₂, amorphous carbon, and SiO₂. The first set of wafers used 80, 300, and 30 nm for the three layers, and was patterned with 193 nm photoresist. Various patterns were available in the mask, and we report here only on arrays of equally spaced lines of 80 and 120 nm and on isolated lines with a nominal width of 120 nm. The average open area of the mask corresponds to approximately 80% of open area. For the second set of wafers, the thicknesses were 50, 100, and 20 nm for the three layers and the wafers were patterned with e-beam resist. The e-beam resist was used to define various patterns on the mask including arrays of lines with varying width and space (from 45 to 100 nm with a step of 5 nm). The e-beam patterned area corresponds to approximately $5 \times 5 \text{ cm}^2$ of the

surface of the wafer, and the remaining of the wafer being patterned by arrays of line and space defined by 193 nm photoresist, resulting in an average open area of approximately 50% on the whole wafer. For all the experiments, the full 300 mm wafers were etched in seasoned chamber conditions, meaning that a thin SiO₂ layer is coated on the chamber walls before the process. The SiO₂, amorphous carbon, and SiO₂ layers are then etched in a three step plasma process with fluorocarbon-based plasma for SiO₂ layers and HBr/Ar/O₂ based plasma for amorphous carbon layer. The remaining amorphous carbon layer is then removed using an oxygen-based plasma and a 3 s-long fluorocarbon-based plasma is used to remove the strip-induced thin oxide from the surface of the silicon. The silicon is finally etched with the HBr/O₂ plasma without additional cleaning or seasoning of the chamber walls to be representative of a real process sequence commonly used in the industry. Figure 1 illustrates the stack and the process flow used for the patterns study.

III. ETCH RATES AND SELECTIVITIES BETWEEN MATERIALS

Blanket wafer studies were carried out to study etch rates and etch selectivities between silicon and SiO₂. The *ex-situ* multipoint automatic ellipsometer is used to give accurate measurements of the amount of etched material, and also to give an estimate of the etch process homogeneity across the wafer because it automatically measures multiple points across the wafer. The homogeneity of the etch rate across the wafer is indicated in the graphs in terms of the standard deviation, σ , from the mean value (in %).

By reducing the duty cycle, the process etch rate is decreased because the averaged ion flux,¹ and very likely also the averaged radical flux,¹⁷ are reduced. To compare etch rates and etched patterns, two concepts can be used. The first one is to compare etch processes with the same amount of total plasma on-time $t_{p,on}$, herein called time compensation (TC). Compared to the process time in the continuous wave (CW) mode, t_{CW} , the pulsed process time, t_p , is extended proportionally with the duty cycle dc to $t_p = t_{CW}/dc$. Therefore, the total plasma on time $t_{p,on} = dc \times t_p$ is equal to the total plasma (on-) time in CW (t_{CW}). In this way, the instantaneous (during the on-time) and the total used plasma power remain the same compared to the CW case. With the concept of time compensation, one can define the time compensated etch rate (TCER) as the etched thickness divided by the total plasma on time. In other words, with ER being the etch rate, $TCER = ER/dc$.

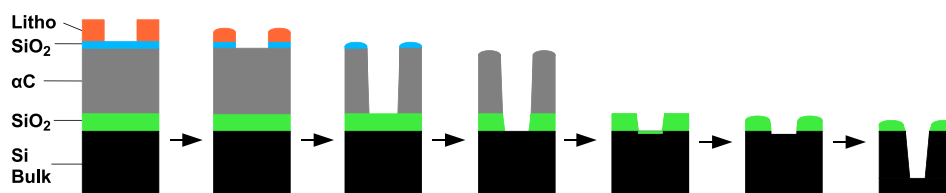


FIG. 1. (Color online) Stack and process flow for the pattern etching.

A second concept, herein named power compensation (PC), should also be mentioned. In this concept, the source power is increased according to the duty cycle to achieve the same average power input as in CW mode to compensate the reduced ion and radical fluxes (the bias power remains constant). Comparable to the TC concept, the power in pulsed conditions is therefore $P_p = P_{CW}/dc$. This leaves the process time as it is, but the plasma itself is greatly changed between different pulse conditions. Even if the ion flux is increased linearly with the source power, the change in ion density will also influence the sheath dynamics close to the target wafer, leading to a decrease in the ion energy.^{18,19} Also, a higher source power increases the degree of dissociation, the plasma neutral species temperature and the relative mixture of plasma species.

In summary, PC changes several parameters at once, making it impossible to clearly identify differences in the process that are only a result of the pulsing. Therefore, only TCER will be discussed in this study.

A. Silicon etching

1. Etch regime

Silicon is thought to be etched by ion enhanced chemical sputtering, leading to the formation of volatile SiBr_xH_y species triggered by energetic ions that supply the needed activation energy and break the Si-Si bonds.^{13,20} Hence, the silicon etching can be limited either by the radical flux and surface coverage (Br, H), or by the ion flux and energy. Figure 2 shows the etch rate in CW mode for different bias powers. Each bias power corresponds to a mean ion energy obtained from the ion energy and flux measurements given in Paper I.¹

The ion flux changes very little with the bias power, and even if the ion energy is cut in half (at a constant ion flux), the etch rate decreases only by 11%. This suggests that in the plasma operating conditions used at 200 W bias power, the etching is essentially working in a neutral limited regime. In other words, the etch rate is primarily controlled by the

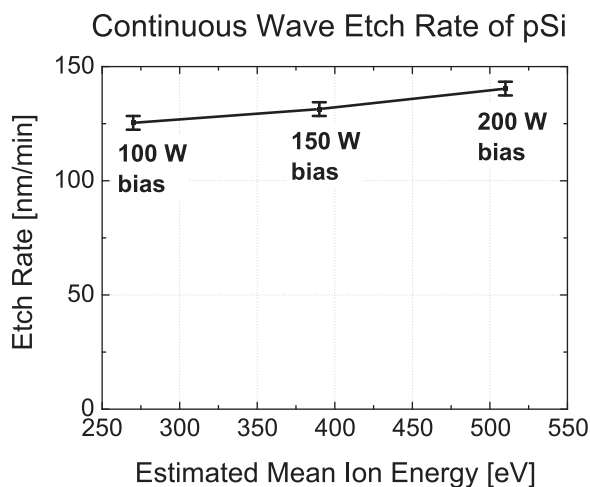


Fig. 2. Etch rate of poly-silicon in a CW process with various bias powers (from blanket wafer experiments).

supply of radicals at the silicon surface and less by the energy brought by the ion on the surface.

2. TCER evolution with the duty cycle

The TCER of poly crystalline silicon (pSi) is shown in Fig. 3 for various duty cycles, including the relative standard deviation, σ , for 25 measurement points across the wafer.

The TCER of pSi increases strongly (up to 60%) at lower duty cycles. Because the silicon etching in our plasma operating conditions seems to be radical-limited, as explained above, this TCER increase is probably linked to an increased availability of Br and H radicals on the Si surface. Although the instantaneous radical flux to the surface is lower in pulsed conditions, the total surface coverage with radicals could be increased with respect to the on-time of the plasma assuming that, during the off-time, radicals accumulate on the surface.

The homogeneity of the etching follows a similar trend. The relative standard deviation decreases with lower duty cycle, indicating a more homogeneous etching attributed to a more uniform radical coverage at lower duty cycles. One possible explanation might be the increased off-time between the plasma pulses where radicals could accumulate on the surface. If the surface coverage of Br becomes more saturated, and therefore more homogeneous, approximately the same amount of silicon can be etched everywhere on the wafer, limiting the impact of the nonuniformity of the radical and ion flux (provided that the etching remains radical limited).

3. TCER evolution with the frequency

Figure 4 shows the TCER of pSi for various frequencies and the relative standard deviation, σ , from the mean value of all 25 measurement points across the wafer. It can be seen that the etch rate increases with the frequency and that the gain increases with decreasing duty cycle, while no significant impact upon σ can be observed. This evolution is discussed in Sec. VC.

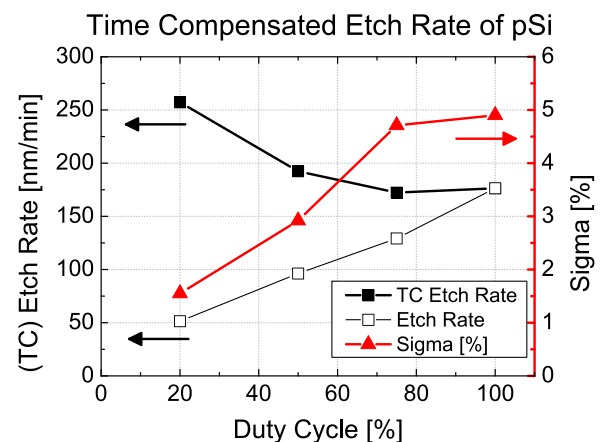


Fig. 3. (Color online) Normal and time compensated etch rates of poly-silicon from blanket wafer experiments for various duty cycles at a frequency of 1 kHz.

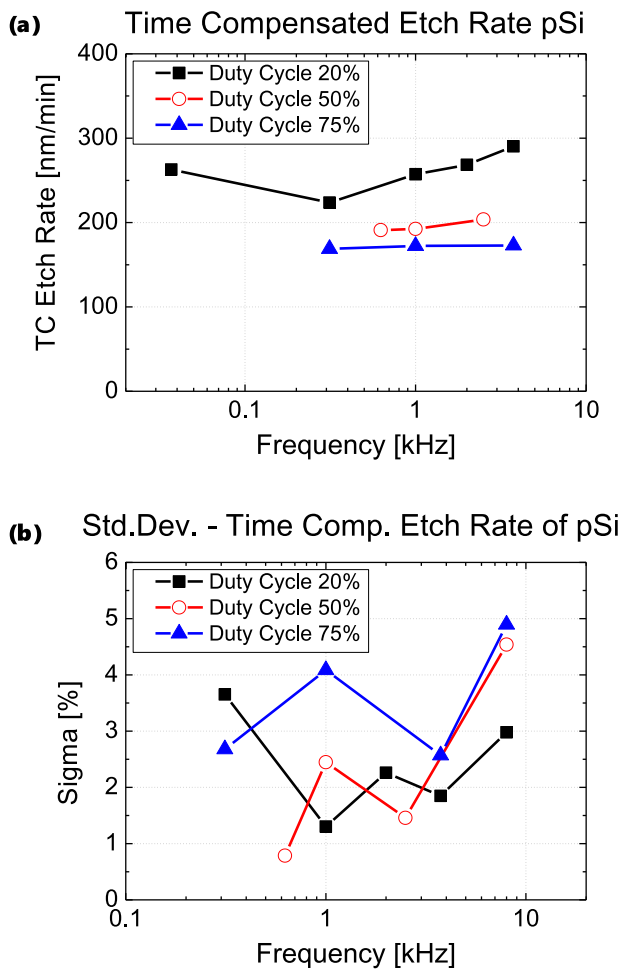


Fig. 4. (Color online) (a) Time compensated etch rate of poly-silicon from blanket wafer experiments for various frequencies and (b) the corresponding relative standard deviation from the mean value.

B. SiO₂ etching

While the silicon etching is thought to be radical limited, the etching of SiO₂ in an HBr/O₂ plasma depends almost exclusively upon the ions because the main etch mechanism is chemical sputtering.^{5,20} Figure 5 shows the dependence of the TCER of SiO₂ upon the duty cycle and the resulting selectivity toward pSi.

The evolution in the SiO₂ TCER can be understood by modeling the evolution of the time compensated etch rate. The results from ion flux and energy measurements¹ for such an HBr plasma indicate that most of the ions have such a low energy that it may not be sufficient to etch SiO₂ in a significant amount.⁵ The flux of highly energetic ions decreases with approximately dc^3 , but at the same time, its mean energy increases. The chemical sputter etch rate is directly proportional to the number of incoming ions, but depends only upon the square root of the ion energy.^{21–25} Assuming that only the high-energy component of the flux contributes to the sputtering of SiO₂ and the threshold energy is negligible compared to the ion energy ($E_{Th} \ll E$), we can calculate the change in ER and TCER at a specific duty cycle, dc , for the average ion flux during the on-time, Γ_p , and the average energy during the on-time, E_p , via

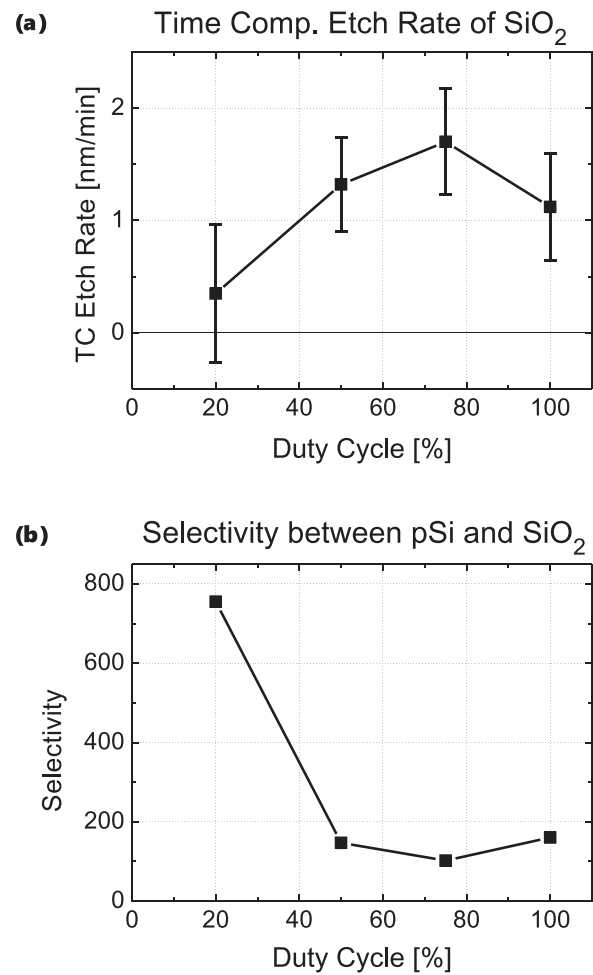


Fig. 5. (a) Etch rate of SiO₂ (mask material) and (b) selectivity of SiO₂ with respect to pSi from blanket wafer experiments.

$$\frac{ER_p}{ER_{CW}} = \frac{\Gamma_p}{\Gamma_{CW}} \cdot \sqrt{\frac{E_p}{E_{CW}}} \quad \text{and} \quad \frac{TCER_p}{ER_{CW}} = \frac{1}{dc} \cdot \frac{\Gamma_p}{\Gamma_{CW}} \cdot \sqrt{\frac{E_p}{E_{CW}}}, \quad (1)$$

where the subscripts p and CW indicate pulsed and continuous wave parameters.

The resulting evolution, based on the data from Ref. 1, is shown in Fig. 6 with $ER_{CW} = 100\%$, and the approximated evolution of the normalized etch rate follows the same evolution as observed for the SiO₂ TCER in Fig. 5(a). Although the plasma conditions are quite different for the ion energy and ion flux measurements (10 mTorr, 1200 W source power, 60 W bias power), we assume that the relative evolution with a change in duty cycle is comparable. The great differences in the etching mechanisms of Si (with a high chemical component) and SiO₂ (mostly physically etched) that were discussed in the introduction lead to a strong increase in selectivity at lower duty cycle values.

IV. REACTIVE ETCH LAYER

The interaction of the plasma process with the wafer is analyzed via x-ray photoelectron spectroscopy. The immediate impact of the plasma etching can be observed in the

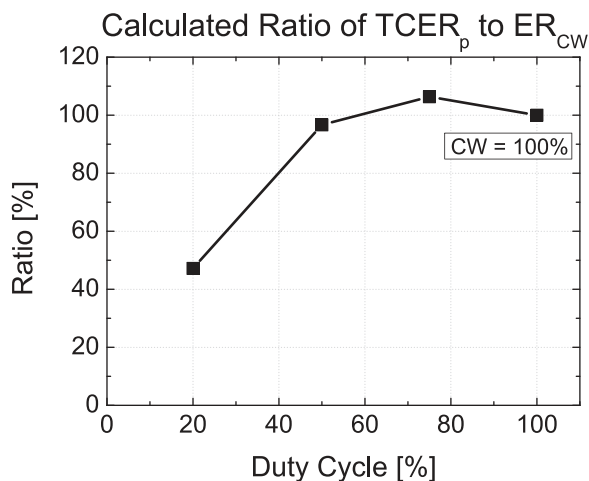


FIG. 6. Approximated sputter yield evolution compared to continuous wave (100%) results based on the change of high energy ion flux and its mean energy.

reactive etch layer that is formed on the silicon surface owing to ion enhanced etching reactions of the modified silicon surface and, depending upon the ion energies, the disturbed layer can exhibit thicknesses up to several nanometers.^{12,26,27} Although the layer is heterogeneous with a continuous change in chemical composition, information on the relative thickness can be obtained from the measured percentage of the bulk silicon, where a greater amount of measured intact bulk silicon (in crystal structure) means a thinner the reactive etch layer. Figure 7 shows the chemical composition of the XPS signal at an angle of $46.25^\circ \pm 3.75^\circ$ from the REL for various pulsed plasma conditions. The contribution of the bulk silicon increases significantly for duty cycles lower than approximately 50% at constant frequency, indicating a decrease of the REL thickness. Only very small differences are observable with increasing frequency at a constant low duty cycle of 20%. It is difficult to identify significant trends for the other elements in the chemical composition because their percentages and variations are very small.

The REL is formed by the ion-neutral synergy that mixes the top silicon surface, breaking Si–Si bonds and inducing the formation of silicon bonded to bromine, hydrogen, and oxygen. When a steady state etch rate is reached, a balance is obtained between chemical sputtering of the modified silicon layer and the propagation of the reactive layer through the silicon bulk. It should be noted that for a thick REL, the ion energy is mainly dissipated in the REL, thereby limiting ion induced mixing reactions in the underlying silicon bulk. In summary, it is known that the REL evolution is a function of plasma operating conditions:²⁸

- (1) An increase in ion energy (or ion flux) will increase the REL thickness because the penetration depth (of ions) and the amorphization will increase. Furthermore, the etch reactions become more ion assisted, leaving behind a reactive layer strongly perturbed, rough and not saturated in halogen based elements.
- (2) An increase in the radical flux at constant ion flux and energy will increase the formation of volatile products, leaving behind a thinner reactive layer.

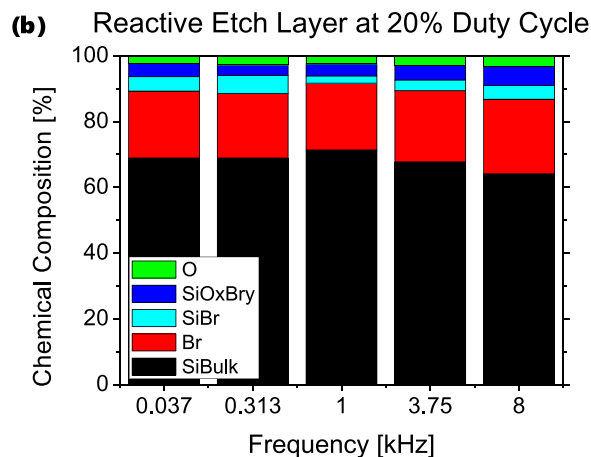
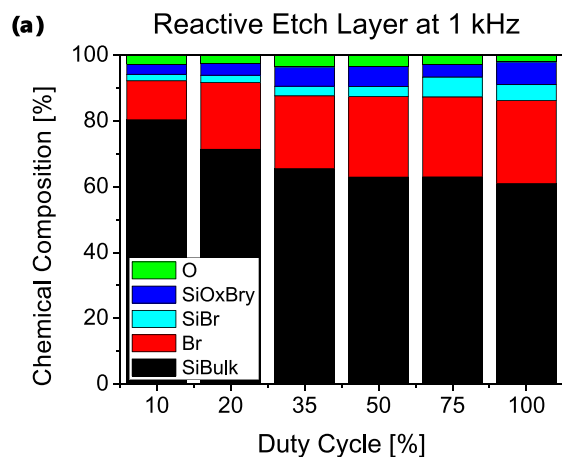


FIG. 7. (Color online) (a) Chemical composition of the XPS signal (at 46.25°) from the reactive etch layer for different duty cycles (at 1 kHz) and (b) frequencies (at 20% duty cycle).

In the present case, we assume that the ratio between the time-averaged radical flux toward the surface and the on-time of the plasma is strongly enhanced at lower duty cycles. In other words, the effective amount of radicals on the surface that is available during the on-time of the plasma is increased. At the same time, the ion flux and mean ion energy is reduced.¹ So, the ratio between the radical and ion fluxes is largely increased at a low duty cycle and the REL thickness decreases accordingly.

Oxygen radicals could have a negative impact upon the etch rate and the REL thickness because they reoxidize the surface by forming SiO_x layers,^{5,9,11,20} and thereby increase the stability of the REL. However, the percentage of measured oxygen is very low in all conditions, indicating that its impact is of minor importance for the REL.

V. SILICON PATTERN ETCHING WITH AN OXIDE MASK

Based on the presented data, we now discuss and explain the differences of pulsed silicon pattern etching with an SiO₂ hard mask from that of the CW process.

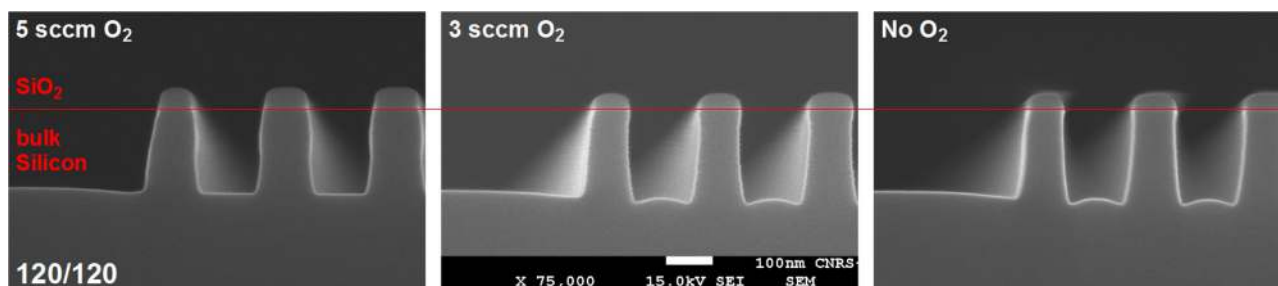


FIG. 8. (Color online) Dependence of the etched patterns with dimensions of 120 nm for the lines and spaces upon the oxygen flow in continuous wave mode.

A. Influence of the oxygen flow

Initially, the impact of the oxygen flux upon the etching of the bulk silicon in CW mode is investigated. The resulting etch profiles containing patterns with nominal dimensions of 120 nm for the lines and spaces are presented in Fig. 8, and actual measured dimensions of the profiles are listed in Table I.

At a reduced oxygen flow, bowed sidewalls can be observed, indicating an increased erosion rate of silicon. This is attributed to a decreased formation of the SPL that is formed by nonvolatile etch products. Oxygen plays a major role to form, harden, and protect this layer from erosion by aggressive radicals formed in the plasma gas phase.^{5,29–31} Without an external oxygen flow, however, the only oxygen sources are the SiO₂-covered reactor walls, the oxide mask and possible residual oxygen concentration in the wafer, which seems to be insufficient to protect the sidewalls from lateral etching. A detailed study on the sidewall passivation layer will be given at the end of this article.

Another aspect is the increased consumption of the oxide mask for lower oxygen fluxes. If more oxygen is available, it is more likely that the surface is reoxidized and SiO₂ bonds are rebuilt before volatile SiBr_x species are created. Also, the mean ion energy is increased in the case without oxygen,¹ which leads to a higher chemical sputtering rate of SiO₂.

Finally, the different geometry and a lower oxidation of the silicon REL in combination with the increased ion energy¹ may lead to the emerging microtrenching.

B. Influence of the duty cycle

In the etch process, the duty cycle is expected to have a rather large influence upon the profiles, considering the results already presented. In Fig. 9, two different patterns are presented etched at a frequency of 1 kHz and various duty cycles, comprising isolated lines with a nominal width of

TABLE I. Measured dimensions of the etched profiles presented in Fig. 8.

Oxygen flow (sccm)	Etched Si depth (nm), ±3 nm	Remaining SiO ₂ mask (nm), ±3 nm	Mean sidewall angle (deg), ±1 deg
5	183.6	44.4	85.6
3	190.2	36.9	86.7
0	190.7	36.9	85.8

120 nm and a pattern with a line and space width of 80 nm. Also, measured dimensions of the profiles are listed in Table II. For a better comparison, time compensated processes are used (identical total plasma on-time), and in addition, the isolated patterns are shown after an HF bath that removes the remaining oxide mask and the sidewall passivation layer. Each observed feature will be discussed individually in the following.

1. Etch rate

By reducing the duty cycle, the TCER is increased, similar to the observation on blanket wafers. As explained previously, this is probably related to the increased availability of etch radicals reaching the silicon surface during the OFF time that then contribute to the etch yield increase during the ON time.

2. Faceting and consumption of hard mask

The oxide mask is less consumed and faceted at low duty cycle since the etching of SiO₂ is mostly triggered by chemical sputtering. The TCER increases slightly for a duty cycle of 75% and decreases strongly afterwards, and as a result, the selectivity between Si and SiO₂ is strongly enhanced. The results from the blanket wafer etching presented at the beginning of this article are in a very good agreement with this behavior.

3. Slope of the etched profile

By decreasing the duty cycle, the slope of the etched profiles becomes more and more vertical, which can be attributed to a thinner SPL on the etched isolated lines. The SPL is created by nonvolatile Si species that adsorb on the sidewalls and react with oxygen to form stable SiBr_yO_x like layers.^{29–32} Analysis of the patterns etched in CW plasma with a lower flux of oxygen (Fig. 8) confirms that the oxygen concentration controls the deposition of the passivation layer. The thinner passivation layer observed at low duty cycle therefore indicates that less oxygen radicals are available to combine on the sidewall surface at low duty cycle. Moreover, the increased availability of etch radicals may lead to more volatile etch products (with lower sticking coefficients), so that the formation of the SPL is further reduced. In addition, these etch products are less redissociated in the plasma gas phase and, thus, are less redeposited in pulsed

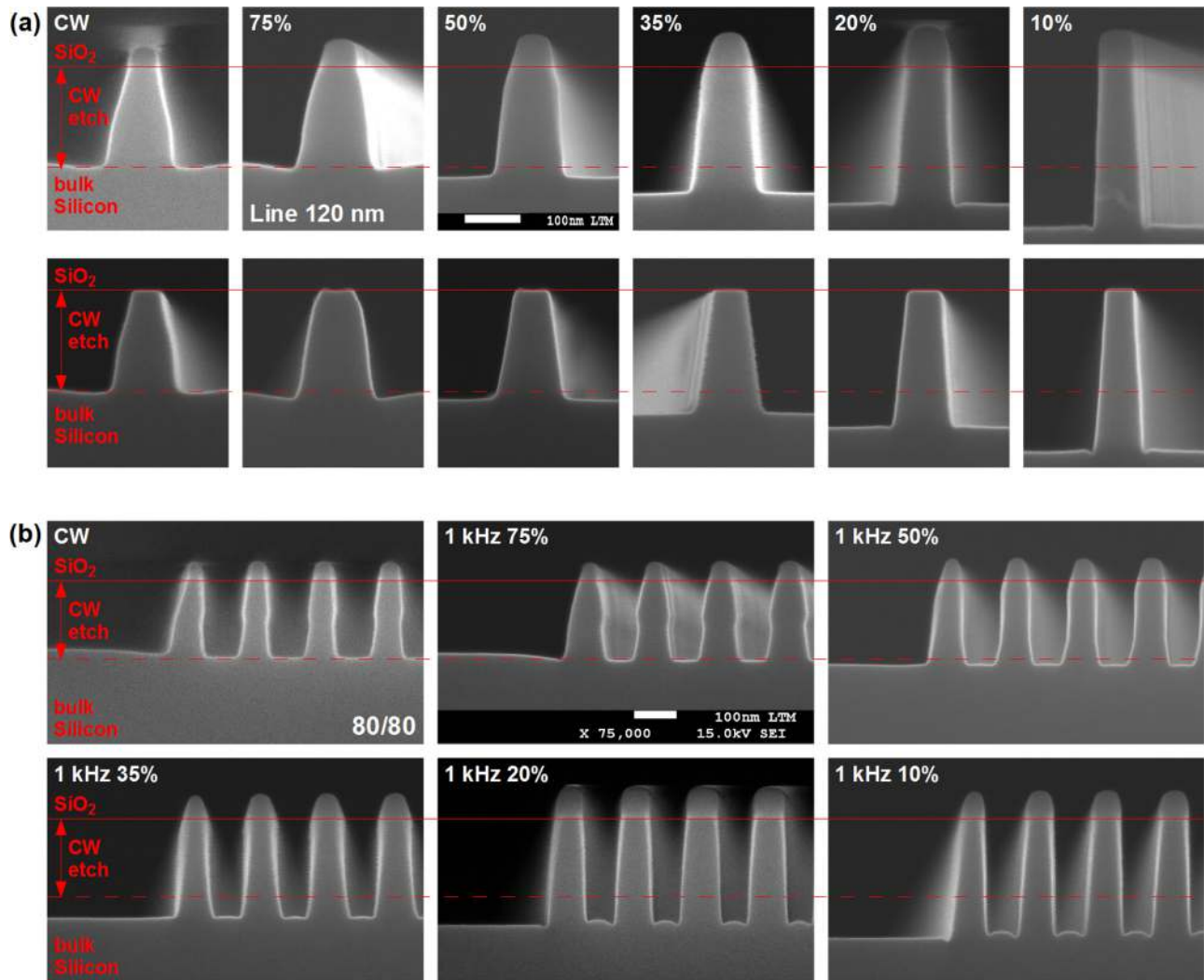


Fig. 9. (Color online) Dependence of the etched patterns upon the duty cycle. (a) Profiles of isolated lines with a nominal width of 120 nm before (top) and after (bottom) HF bath. (b) Profiles of nested pattern with a line and space width of 80 nm.

TABLE II. Measured dimensions of the etched profiles presented in Fig. 9.

Pattern	Before/after HF bath	Duty cycle (%)	Etched Si depth (nm), ± 3 nm	Remaining SiO ₂ mask (nm), ± 3 nm	Mean sidewall angle (deg), ± 1 deg
Line 120	Before	CW	180.8	37.9	78.4
Line 120	Before	75	185.5	46.7	79.0
Line 120	Before	50	201.4	56.1	82.6
Line 120	Before	35	224.8	59.8	84.8
Line 120	Before	20	245.3	76.2	87.6
Line 120	Before	10	282.2	67.8	87.6
Line 120	After	CW	184.6		78.8
Line 120	After	75	193.0		78.9
Line 120	After	50	195.3		80.4
Line 120	After	35	222.0		81.4
Line 120	After	20	245.3		84.4
Line 120	After	10	286.0		86.0
80/80	Before	CW	185.5	38.8	85.0
80/80	Before	75	188.3	45.3	82.8
80/80	Before	50	196.7	51.9	85.1
80/80	Before	35	228.5	59.8	87.0
80/80	Before	20	240.7	72.9	86.8
80/80	Before	10	275.7	68.2	88.5

plasmas. More details on the formation of the SPL will be given in Sec. VI.

4. Profile difference in open/dense patterns

In CW mode, a large difference between open and dense profiles can be observed. The larger collection angle for neutral species from the gas phase can increase the amount of deposited material on open (exposed) sidewalls, and by decreasing the duty cycle, this effect of aspect ratio-dependent etching is reduced. In a plasma pulsed at a frequency of 1 kHz and a duty cycle of 20%, open and dense profiles become almost identical and, because the SPL thickness is reduced everywhere (as explained above), the absolute differences between open and dense pattern structures are also reduced, even though the relative difference may still be the same.

5. Microtrenching

Two shapes for the microtrenching can be observed on our SEM images, with a very “broad” microtrenching that is especially visible close to isolated patterns, and a “narrow” microtrenching that is especially visible in narrow trenches. In both cases, the etched depth is slightly larger close to the foot of the patterns, but this slightly deeper etching extends laterally on ~ 120 nm for the “broad” microtrenching, while it extends only on ~ 15 nm for the “narrow” microtrenching.

The broad microtrenching can be explained by the gas phase deposition of species that slow down the etching, such as oxygen radicals forming SiO_x (Refs. 5, 9, 11, and 20) or redissociated etch by-products. In areas with small collection angles (close to the patterns), less etch-inhibiting species are deposited and the etch rate is larger. Note that this effect is expected to be less important for less sticking bromine containing species that can more easily reach the foot of the patterns after colliding on the pattern sidewalls or by surface diffusion. In combination, this leads to the broad microtrenching. With decreasing duty cycle, the radicals can accumulate and diffuse on the surface during the off-time, leading to a more homogeneous radical availability and therefore to more uniform silicon etching (except for the narrow microtrenching that is explained later). In addition, the redissociation and subsequent deposition of etch by-products are reduced, which further counters the formation of the broad microtrenching. Therefore, we explain the reduction of the broad microtrenching at low duty cycle by a reduction of the availability of etch inhibitors and an improvement of the uniformity of the bromine concentration at the etch front thanks to the longer off time.

The narrow microtrenching in dense structures could be explained as follows: In a purely geometrical view, more vertical and less bowed sidewalls, observed at lower duty cycles, lead to a focus of scattered ions close to the sidewall.^{33–36} In addition, the radical (Br) to ion flux ratio increases at low duty cycle, leading to conditions in which the etching becomes more and more affected by the ion flux and energy. In this case, the etch rate may be more susceptible to a local increase in the ion flux at the edges of the

pattern, where ions are focused by scattering on the sidewalls. Finally, charging effects, which are expected to be reduced in pulsed plasmas,^{37–42} might also play a role concerning the microtrenching.^{34,43} Therefore, we explain the narrow microtrenching at low duty cycle by the focusing of the ions close to the foot of the pattern and the shift toward a more ion limited regime.

6. Exception at 10% duty cycle

The only exception to the overall evolution can be observed for the profiles obtained at 1 kHz and 10% duty cycle. Compared to a duty cycle of 20%, the mask is more consumed and faceted, indicating an increase in physical sputtering. A similar effect can also be seen by going to high frequencies, which will be discussed in the following.

C. Influence of the frequency

The plasma diagnostic data indicate an influence of the frequency at low duty cycles. In Fig. 10, the impact of the frequency is shown for etch processes at duty cycles of 75%, 50%, and 20%, up to a frequency of 8 kHz. The profiles shown are obtained from patterns with a line and space width of 120 nm. Again, measurements of the amount of etched silicon, the thickness of the remaining SiO₂ mask and the average sidewall angle are listed in Table III.

The impact of the frequency can clearly be seen on the three series of SEM images. By increasing the frequency up to a certain limit that is dependent upon the duty cycle, no significant change in the etched profiles is observable. For higher frequencies beyond this limit, the etch rate starts to increase not only for silicon but also for the oxide mask that leads to an increased faceting of the hard mask. This was also observed in Sec. III A 3.

For a lower duty cycle, the limiting frequency decreases. It is possible that the pulsed etching at 1 kHz and 10% duty cycle is already in this limit, which could explain the differences from the general evolution with respect to the duty cycle.

In general, the impact of the frequency can be detected at a combination of high frequency and low duty cycle. In these conditions, the power matching of the plasma etch process is very difficult, indicating unstable plasma conditions. The point where the frequency impact can be detected might be correlated to the on-time of each pulse, which is indicated on the top right of several SEM images. Below a threshold value of approximately 100 μ s, the frequency impact can be observed, potentially linked to a highly transitional plasma regime at the beginning and end of the pulse. The comparison of the characteristic time constants of certain plasma parameters can give a better understanding of this phenomenon.

In Fig. 11, the time-resolved ion flux in a pulsed HBr/O₂ plasma at 1 kHz and 10% duty cycle is shown, obtained with a capacitive ion flux probe.¹ In principle, the ion flux in a electronegative plasma is approximately equal to the Bohm flux $\Gamma_{\text{Bohm}} = n_i \cdot \sqrt{k_B T_e \cdot (1 + \alpha_S) / m_i (1 + \alpha_S \eta)}$, with $\alpha_S = n_{i-} / n_e$ and $\eta = T_e / T_{i-}$. Here, the subscripts *i* and *e* indicate parameters from ions and electrons, k_B is the Boltzmann

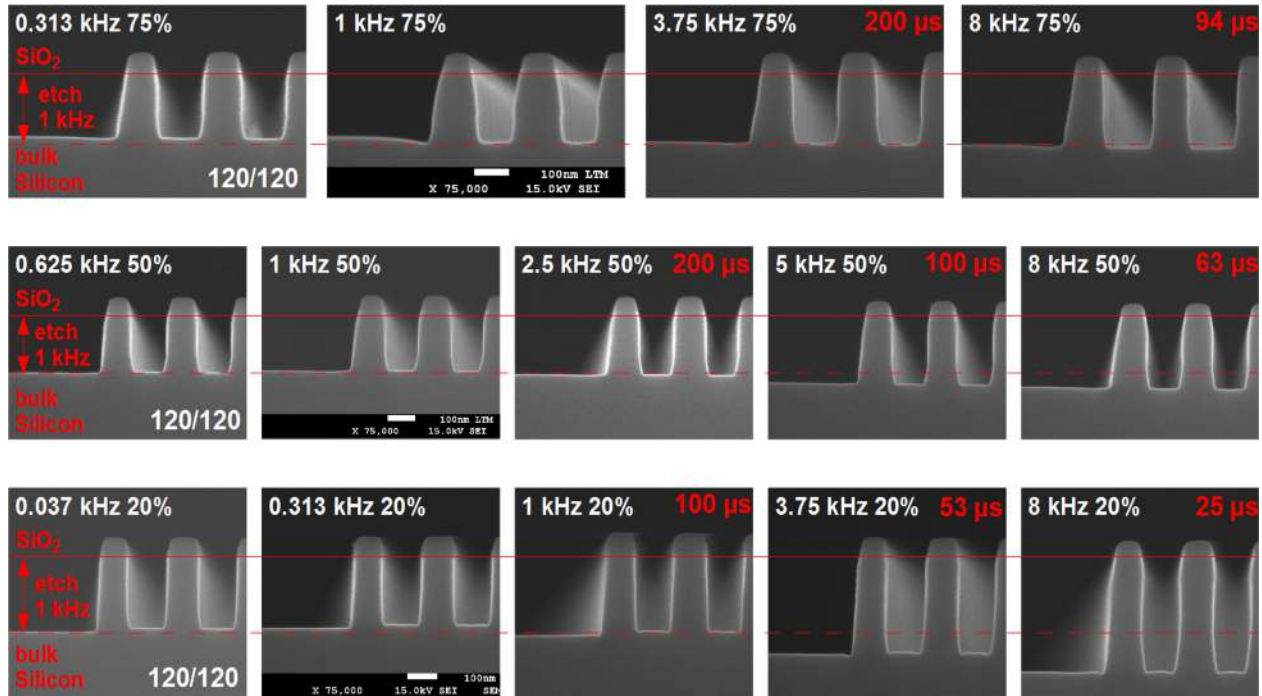


FIG. 10. (Color online) Dependence of the etched patterns upon the frequency. The profiles come from patterns with a line and space width of 120 nm. The etch conditions are indicated on the top left and, for certain images, the plasma on-time of each pulse is indicated in red on the top right.

constant, T is the temperature, n is the density, and m is the mass.

The influence of the electron temperature, T_e , and the ion density, n_i , upon the ion flux can be distinguished, where at the beginning and the end of the pulse the ion flux “jumps” because of a fast change of the electron temperature in a time scale of 20–30 μs , and the change in ion density is significantly slower. At low duty cycle and high frequency, the short on-time of each pulse approaches the time scale of the highly transitional plasma regime during which the electron temperature is not in equilibrium. Consequently, the time during which the etch proceeds in the highly transitional regime becomes non-negligible compared to the total on-time of the plasma. A further increase in frequency also increases

the importance of the etching in the transitional regime. Consequently, etched profiles cannot be compared any more under a time compensated view because the ratio between the transitional regime and normal regime may change between two etch conditions. To understand the characteristics of the transitional regime, further experiments would have to be carried out.

D. Comparison to smaller pattern profiles

In the previously presented experiments, etch results are examined for large patterns, and in the following, these results are compared to profiles with smaller dimensions down to 45 nm-wide trenches. The stack materials and the

TABLE III. Measured dimensions of the etched profiles presented in Fig. 10.

Frequency (Hz)	Duty cycle (%)	Etched Si depth (nm), ± 3 nm	Remaining SiO ₂ mask (nm), ± 3 nm	Mean sidewall angle (deg), ± 1 deg
0.313	75	182.2	45.8	85.9
1	75	190.2	49.5	82.6
3.75	75	193.7	49.8	85.8
8	75	204.2	39.7	85.7
0.625	50	197.2	55.1	85.7
1	50	196.3	57.9	84.9
2.5	50	211.7	50.5	85.9
5	50	236.5	45.8	85.4
8	50	245.3	43.0	85.2
0.037	20	221.5	60.3	88.4
0.313	20	205.6	65.4	88.5
1	20	233.2	69.6	87.6
3.75	20	296.3	64.0	87.3
8	20	358.4	46.7	87.0

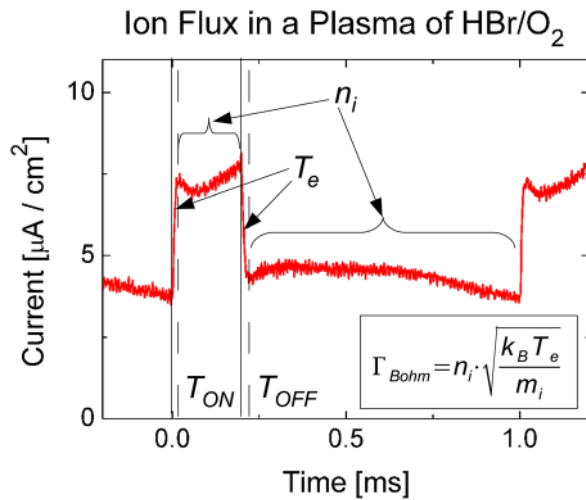


FIG. 11. (Color online) Time resolved ion flux in a pulsed HBr/O₂ plasma at 1 kHz and 10% duty cycle obtained from a capacitive ion flux probe (Ref. 1). The influence of a change in the electron temperature, T_e , and the ion density, n_i , upon the ion flux evolution is indicated.

process flow are the same as those in the oxide mask experiments, but the thickness of the mask layers is reduced to ensure that the thinner lines are stable enough and do not collapse. In addition, the open ratio of the mask changed from $\sim 80\%$ to $\sim 50\%$. In consequence, the mask etching steps are shorter, and the resulting chamber wall conditions might be slightly different to the walls conditions of the previous experiments.

Electron beam lithography is used to achieve these small structures and, in Fig. 12, etched lines and trenches are shown with changing dimensions from 45 nm on the outside to 100 nm in the middle for CW and pulsed conditions. Neighboring trench and line dimensions differ by 5 nm so that a possible reactive ion etch (RIE) lag could be easily observed.

The only differences compared to the previous stack and patterns are the strong microtrenching and the bowed sidewalls at a duty cycle of 10%. Even at a 20% duty cycle, the microtrenching and a very light bow are observable. The general trends, however, are the same as before, wherein a lower duty cycle increases the Si TCER and reduces the faceting and consumption of the mask (except for a 10% duty cycle), leading to the appearance of microtrenching and to a change of the sidewall slope owing to a reduced formation of the SPL. The discrepancy between these and the larger patterns may be owing to the different mask coverage and to the different amounts of previously etched layer materials that could influence the reactor wall coating.

In all cases, no RIE lag is observed.

VI. SIDEWALL PASSIVATION LAYER ANALYSIS

One of the most important features observed in pulsed plasma conditions is the profile evolution that can be attributed to the formation of a modified sidewall passivation layer. Oehrlein *et al.*²⁹ proposed a model of the formation of

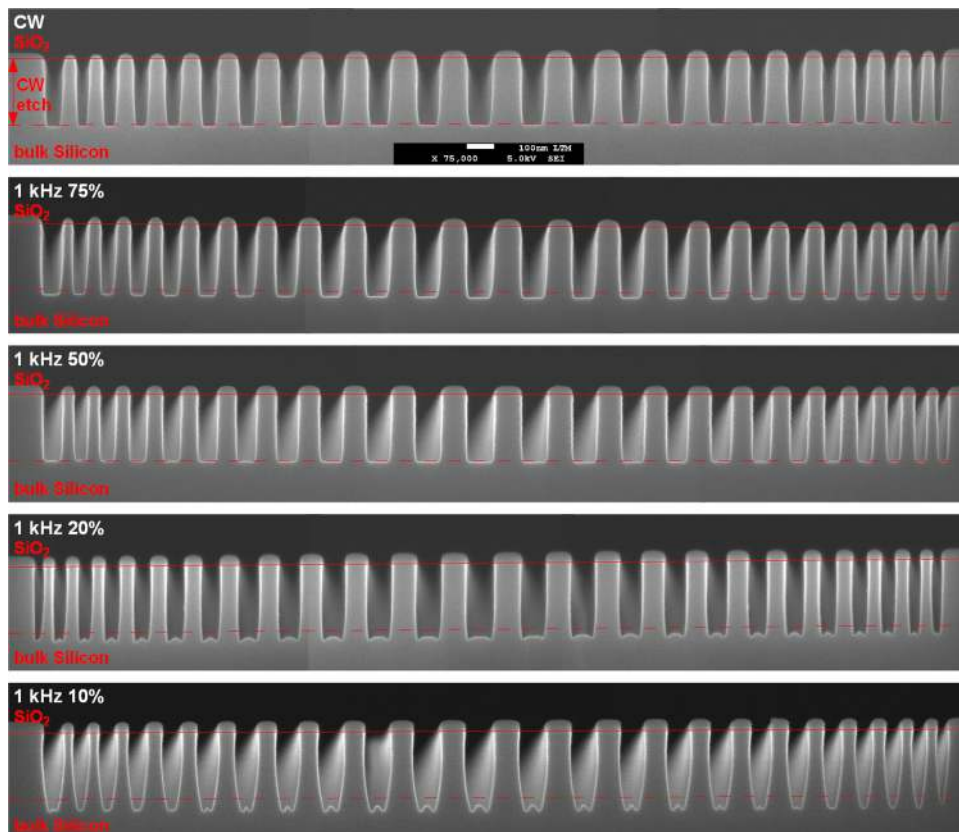


FIG. 12. (Color online) Etched Si patterns with changing trench dimensions from 45 nm on the outside to 100 nm in the middle with a step size of 5 nm for continuous wave and pulsed conditions.

the sidewall passivation layer. At first, species from the silicon surface that are chemically sputtered at off-normal angles reach the pattern sidewalls in the same state as when they left the etched surface (line-of-sight deposition). Often, these sputtered species are nonvolatile and should have a high sticking probability. Because the ion bombardment is very limited at the sidewalls, these species remain adsorbed for a relatively long time, and similar species could also be deposited from the gas phase after dissociation of volatile etch products. Reactive oxygen species in the plasma interact with the adsorbed molecules and form oxide-rich silicon compounds (formation of SiO₂ is thermodynamically favored). Based on this model, the formation of the SPL can be either limited by the oxygen flux from the gas phase or by the deposition of nonvolatile silicon species. The neutral flux from the gas phase is correlated to the aspect ratio of the pattern (collection angle), and the line-of-sight deposition is linked to the sputter angle distribution and the width of the etch surface (trench bottom).

To study the chemical composition and the thickness of the SPL in a quasi *in-situ* fashion, an XPS technique was developed that is described in detail in a previously published article.⁴⁴ For such an investigation, a special pattern with equal line and space widths is needed. In this work, multiple 1 × 1 mm arrays of line = space patterns are used

with a critical dimension of 45–100 nm produced by electron beam lithography.

In this particular case, quasi *in-situ* analyses are important because bromine could be exchanged by oxygen in the SPL if exposed to the atmosphere^{5,10,11} or to low pressure conditions where oxygen is present.

A. Thickness profiles

The thickness profiles from the SPL analysis are shown in Fig. 13 for various trench dimensions in different pulsed conditions. In general, the SPL thickness decreases when the aspect ratio increases. Note that for a CW plasma, the thickness of the SPL also decreases close to the top of the features because of the faceting of the mask. The SPL thickness seems to depend only upon the aspect ratio, and not upon the probed trench depth or the trench width. This also means, however, that the SPL thickness does not (strongly) depend upon the exposure time to the plasma, which means that the SPL might be controlled by a dynamic equilibrium. Based on these results, the thickness profiles are considered to be independent of the trench dimensions within the margin of error present, and averaged profiles are used for comparison between different plasma etch processes.

As explained above, the model given by Oehrlein *et al.*²⁹ suggests two mechanisms that alone or in combination lead

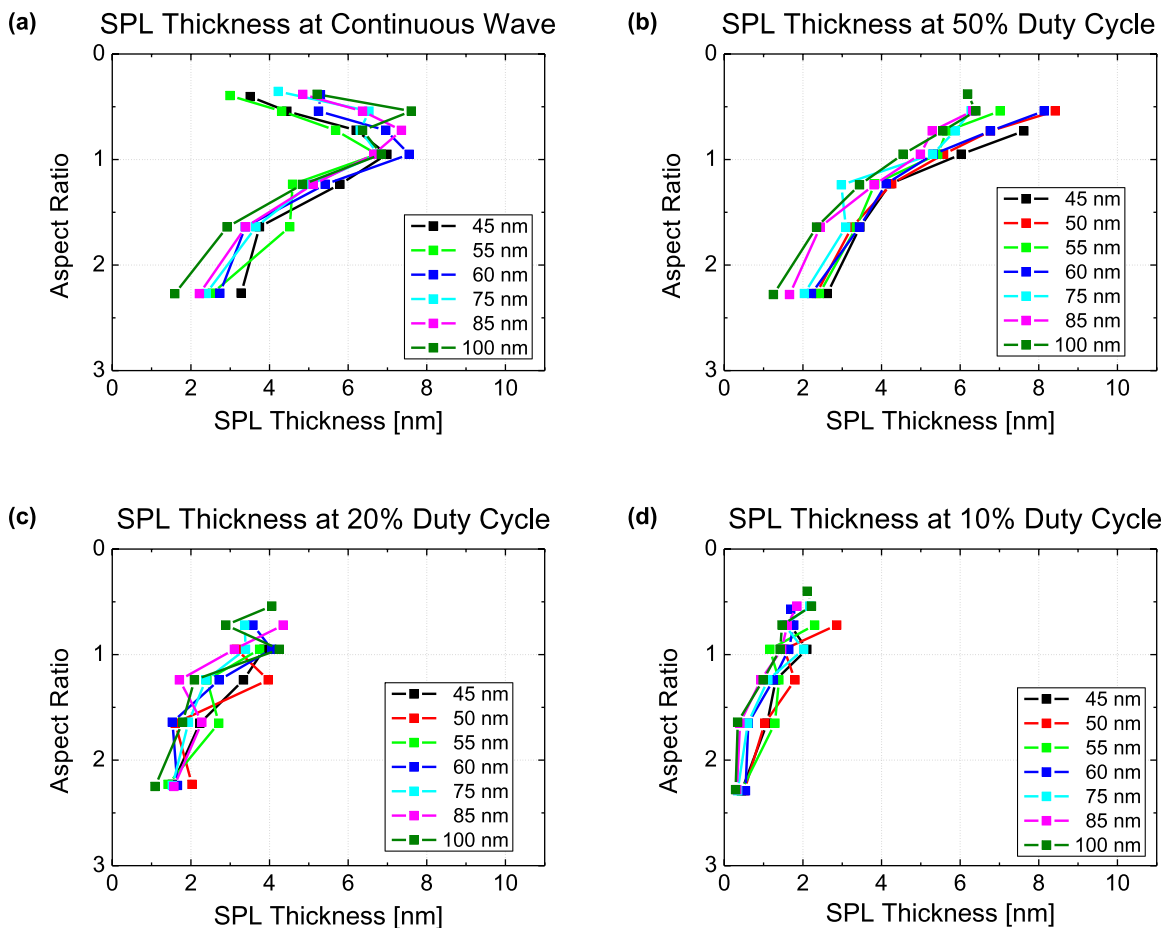


FIG. 13. (Color online) Sidewall passivation layer thickness obtained from XPS results for pulsed etching of different trench widths at continuous wave and at 1 kHz with various duty cycles. Parts (a) and (b) were reprinted with permission from M. Haass *et al.*, *J. Appl. Phys.* **111**, 124905 (2012). Copyright 2012 American Institute of Physics.

to the formation of the SPL. The flux may come from the gas phase (radicals or etch products) or from a line-of-sight deposition of strongly sticking, nonvolatile sputtered species.

Hübner⁴⁵ developed a simplified analytical model to describe the deposition on the sidewalls by both processes. His models are based on geometrical considerations for both mechanisms and estimate the deposition rate and the final thickness along the height of the pattern. In Fig. 14, the resulting sidewall passivation thicknesses are shown for either gas phase deposition only or line-of-sight deposition of sputtered etch products only.

The modeled profiles differ strongly. For the gas phase deposition, the aspect ratio is the main factor with a small dependence upon the trench width also visible, where wider trenches lead a thinner SPL at a constant aspect ratio because the exposure time to the plasma is reduced in this case.

The direct deposition of sputtered species, on the other hand, depends strongly upon the trench width and not upon the aspect ratio. This is quite clear because a larger trench offers more material that can be sputtered and deposited on the sidewalls, so the SPL thickness increases with wider trenches at a constant depth.

While the model for the line-of-sight deposition is very different than the experimental results, the gas phase deposition model resembles the observed thickness profiles to some extent. Thus, we may assume that the formation of the SPL in our conditions is owing to a combination of both mechanisms, where unsaturated, strongly sticking, silicon-containing etch products adsorb on the sidewalls and are transformed into a protective layer if they are oxidized by O radicals from the gas phase. This model is quite similar to the formation of passivation layers in an HBr/Cl₂/O₂ plasma.⁴⁶

Figure 15 shows the average SPL thickness profile for various pulsed conditions and for the CW mode with two oxygen flow values. For a better visualization, the theoretical error⁴⁴ is not included.

With decreasing duty cycle at a constant frequency of 1 kHz, the overall thickness of the sidewall passivation layer decreases significantly. The reduced SPL thickness explains the more vertical etch profiles and partially explains the reduced differences between dense and open patterns, as noted in Sec. V. The decrease of the SPL thickness for small aspect ratios (top of the trenches) in CW mode is owing to a strong mask faceting, leaving the top of the sidewalls less protected by the mask (see Fig. 12). Consequently, the top of the SPL is partially eroded, leading to a thinner layer. In a comparable etch process, a similar profile was also found by Detter *et al.*⁴⁷

As the aspect ratios become larger, the SPL decreases continuously because of the reduced collection angle.

The reduced thickness of the SPL with lower duty cycles could be linked to either a lower time compensated flux of highly sticking silicon species or to a reduced time compensated flow of oxygen radicals (or a combination of both), as discussed above. At a lower duty cycle, the time compensated Br radical availability on the surface is likely to be

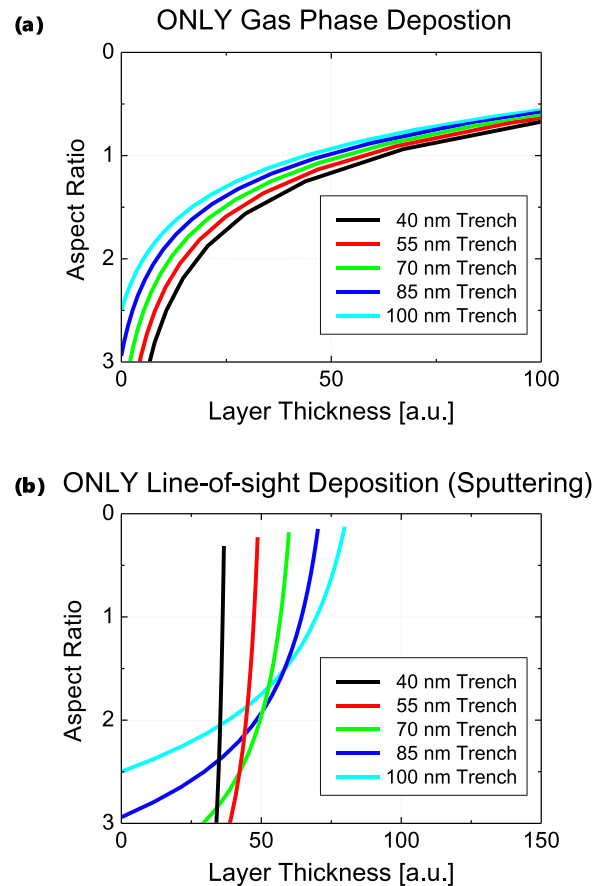


FIG. 14. (Color online) (a) Passivation layer thicknesses from model calculations (Ref. 45) for gas phase deposition only and (b) for line-of-sight redeposition of sputtered etch products only. Trench dimensions are chosen close to our pattern dimensions (depth of 240 nm, various trench widths).

increased, so that more Br is available to form volatile etch products. This likely reduces the amount of nonvolatile etch species in the plasma and the direct line-of-sight deposition of partially volatile etch products. In addition, because the overall dissociation in the plasma is reduced, less etch products are redissociated into nonvolatile species that are

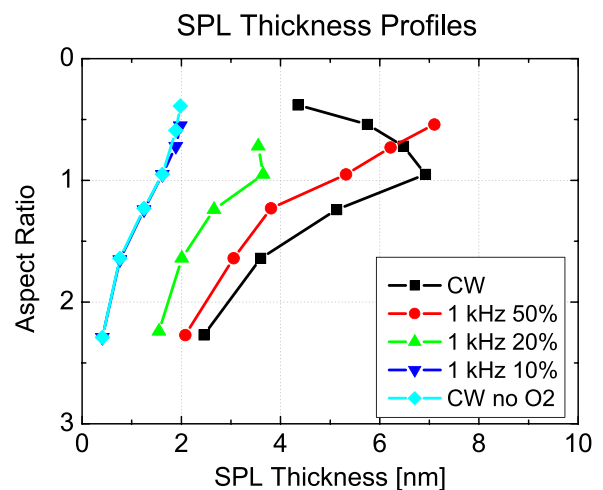


FIG. 15. (Color online) Average thickness of sidewall passivation layer for different duty cycles and continuous wave mode, with and without O₂.

subsequently deposited. Therefore, we suppose that the time compensated flux onto the surface of highly sticking species is reduced, even though the TCER is increased.

For the O radical density, on the other hand, we expect a fast decrease at reduced duty cycles for the following reasons:

- (1) A reduction of the oxygen flow in the CW process results in a strong decrease of the SPL thickness, which suggests that the oxygen limits the SPL formation in this case.⁴⁸
- (2) A decrease of the duty cycle leads to a reduced dissociation of O₂ similar to other molecules (like HBr). The O radicals have a higher sticking coefficient than the Br radicals, replacing Br bonds on the surface and especially on the reactor walls, which are coated with etch by-products containing silicon and bromine. In summary, the oxygen is scavenged more efficiently than bromine, so the O radical availability on the surface for further reactions is more decreased than the Br availability.
- (3) The thickness profiles from CW without oxygen and from the pulsed experiment at 1 kHz and 10% duty cycle are almost identical. This also supports the assumption that oxygen plays a major role in the formation of the SPL in our conditions³¹ and that the SPL thickness is limited by gas phase oxidation.

The same explanation is valid for the results of the pattern comparison with different oxygen flows in Sec. V.

B. Chemical composition profiles

In addition to the SPL thickness, its chemical composition is also analyzed. In Fig. 16, the atomic percentage of oxygen in the SPL is shown with respect to the aspect ratio for pulsed etching at 1 kHz and 10% duty cycle. The amount of oxygen is clearly dependent upon the aspect ratio, but no significant dependence upon the trench dimensions can be observed, similar to the thickness profiles. This is also true for the other elements present in the SPL, namely, silicon

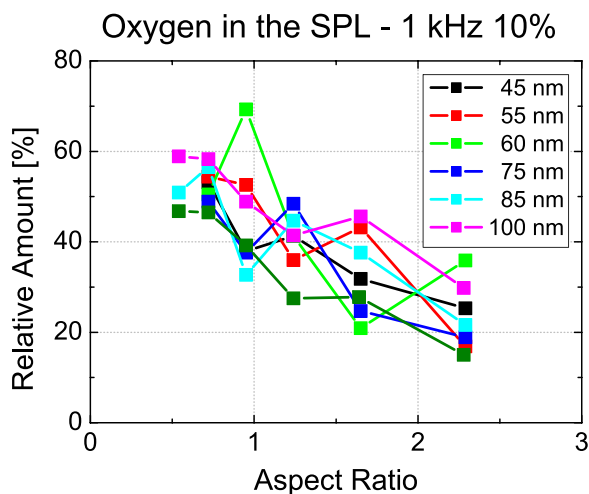


Fig. 16. (Color online) Percentage of oxygen in the SPL for various trench critical dimensions and aspect ratios for pulsed etching at 1 kHz and 10% duty cycle.

and bromine, supporting the assumed formation mechanism discussed above.

For a comparison between etch conditions, the chemical composition for each aspect ratio is therefore averaged over the range of different trench dimensions. In Fig. 17, the mean chemical composition of the SPL is presented without the contribution of the bulk silicon versus the probed aspect ratio.

In all conditions, a decreasing amount of oxygen and an increasing amount of bromine and silicon is observed with increasing aspect ratio. While for almost all aspect ratios and conditions, the ratio of Si to Br remains approximately 1, the ratio of Si to oxygen changes greatly. The evolution of the oxygen amount with the aspect ratio is especially pronounced for pulsing at a low duty cycle and in the CW mode without O₂. In the latter case, oxygen atoms can only be introduced into the plasma by sputtering from the reactor wall (deposited protective layer) or from the oxide mask, leading to a reduced oxygen density. The lower overall oxygen radical flux leads to an SPL that is very sensitive to the collection angle of oxygen radicals and, thus, the aspect ratio, which may lead to the observed reduced amount of oxygen in the SPL at higher aspect ratios.

For pulsing at a low duty cycle, we also expect a reduction of the oxygen radical flux, as explained in Sec. VI A. In addition, the sputtered and etched particles from the surface are thought to be more volatile because they incorporate less oxygen, which leads to a net reduction of the available oxygen in the etched trenches, similar to the case without added O₂ in the gas flow.

VII. SUMMARY—IMPACT OF PLASMA PULSING UPON SILICON ETCHING

The plasma pulsing greatly influences the investigated HBr/O₂ silicon pattern etch process. By reducing the duty cycle, the following profile evolution can be observed and explained:

- (1) The radical-limited, time compensated etch rate of silicon is enhanced because the accumulation of etch radicals during the off-time leads to a net increase of radicals available for the etching with respect to the on-time.
- (2) The faceting and consumption of the mask is reduced owing to a decreased chemical sputtering.
- (3) The slope of the etched profile becomes more vertical owing to a reduced formation of the SPL. Its formation is controlled by a combination of the deposition of highly sticking silicon etch products and by a subsequent oxidation by O radicals from the gas phase, where the latter plays the limiting role. Similar to the effect of pulsing, the modification of the O₂ flow in CW mode can be used to obtain a thinner SPL. However, in CW mode, this layer does not efficiently prevent lateral etch. Pulsing, on the other hand, can be used to obtain almost vertical profiles in a highly selective process.
- (4) The difference between dense and isolated profiles is smaller, which may be linked to a reduced formation of

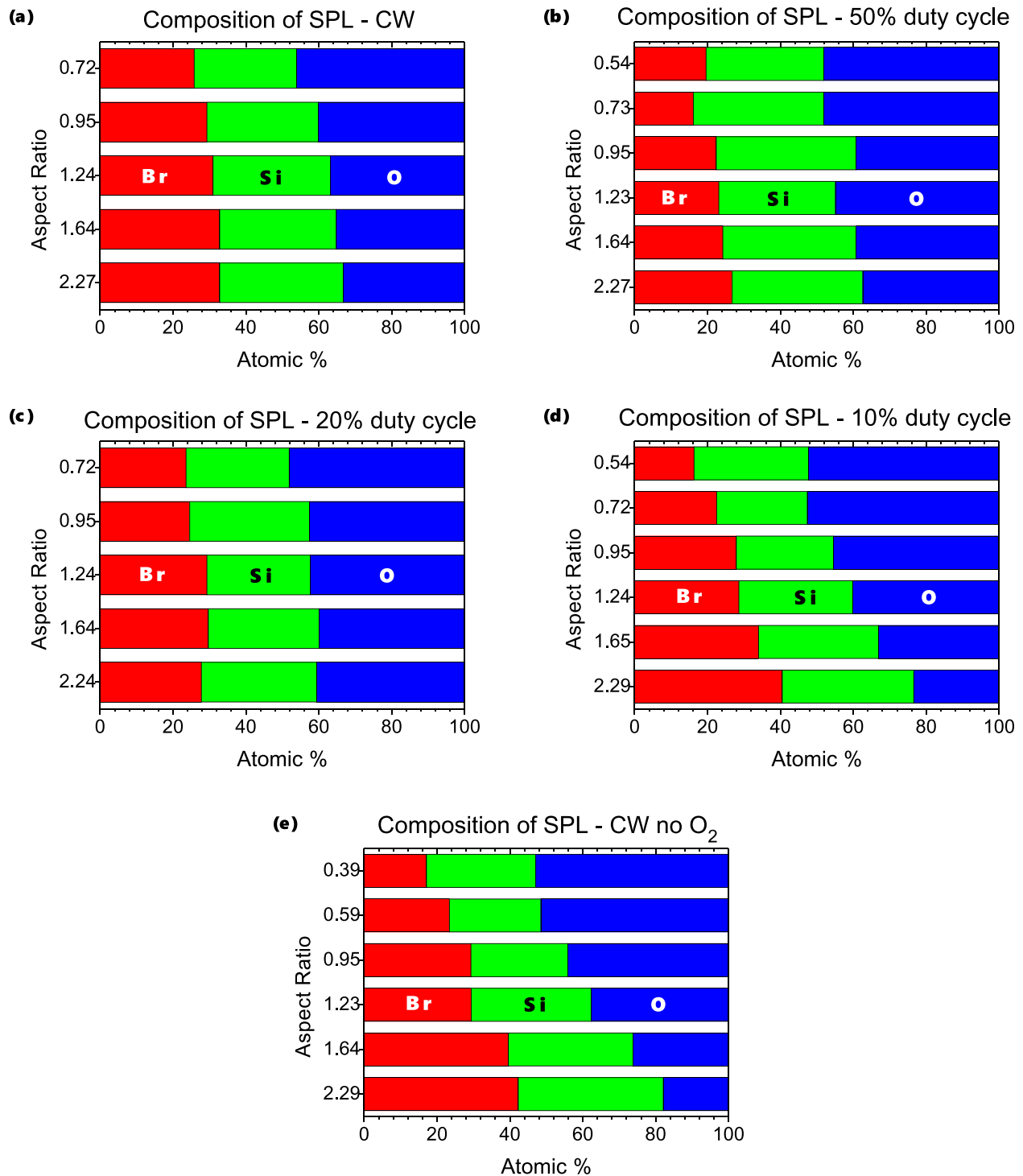


Fig. 17. (Color online) Sidewall passivation layer analysis—average chemical composition for different duty cycles at a frequency of 1 kHz.

the SPL and also to a more homogeneous distribution of neutral species, such as O.

- (5) The broad trenches at high duty cycles and in the CW mode may be linked to the difference in the collection angle for depositing and oxidizing species from the gas phase that inhibit the silicon etching. By reducing the duty cycle, fewer species are deposited, the O radical flux is reduced and the broad microtrenches vanish. In contrast, narrow microtrenching in dense patterns occurs,

especially at lower duty cycles, which is linked to a localized focusing of reflected ions at almost vertical sidewalls and to a higher sensitivity of the etch rate to the ion flux.

In conditions with a combination of a high frequency and a low duty cycle, an impact of an increase of the frequency becomes observable. This is likely owing to the highly transitional plasma regime at the beginning and the end of the

pulse. A decrease of the plasma on-time (equal to an increase in the frequency for a given duty cycle) changes the ratio between the highly transitional and the “normal” plasma regime. Consequently, results from time compensated etching can no longer be directly compared. Moreover, the power matching in these conditions is very difficult with the current reactor equipment.

In summary, pulsed plasmas offer new possibilities to improve the homogeneity and selectivity of and to reduce the impact of the plasma on the etched surface.

ACKNOWLEDGMENT

This work was partially supported by the French National Nanofabrication Network (RENATECH).

- ¹M. Haass, M. Darnon, G. Cunge, D. Gahan, and O. Joubert, *J. Vac. Sci. Technol. B* **33**, 032202 (2015).
- ²C. Petit-Etienne, M. Darnon, L. Vallier, E. Pargon, G. Cunge, F. Boulard, O. Joubert, S. Banna, and T. Lill, *J. Vac. Sci. Technol., B* **28**, 926 (2010).
- ³C. Petit-Etienne, E. Pargon, S. David, M. Darnon, L. Vallier, O. Joubert, and S. Banna, *J. Vac. Sci. Technol., B* **30**, 040604 (2012).
- ⁴C. Petit-Etienne, M. Darnon, P. Bodart, M. Fouchier, G. Cunge, E. Pargon, L. Vallier, O. Joubert, and S. Banna, *J. Vac. Sci. Technol., B* **31**, 011201 (2013).
- ⁵T. D. Bestwick and G. S. Oehrlein, *J. Vac. Sci. Technol., A* **8**, 1696 (1990).
- ⁶V. M. Donnelly, F. P. Klemens, T. W. Sorsch, G. L. Timp, and F. H. Baumann, *Appl. Phys. Lett.* **74**, 1260 (1999).
- ⁷M. Fukasawa, Y. Nakakubo, A. Matsuda, Y. Takao, K. Eriguchi, K. Ono, M. Minami, F. Uesawa, and T. Tatsumi, *J. Vac. Sci. Technol., A* **29**, 041301 (2011).
- ⁸T. Ito, K. Karahashi, S.-Y. Kang, and S. Hamaguchi, *J. Phys. Conf. Ser.* **232**, 012021 (2010).
- ⁹S. Kuroda and H. Iwakuro, *J. Vac. Sci. Technol., B* **16**, 1846 (1998).
- ¹⁰K. Miwa and T. Mukai, *J. Vac. Sci. Technol., B* **20**, 2120 (2002).
- ¹¹M. Nakamura, K. Koshino, and J. Matsuo, *Jpn. J. Appl. Phys.* **31**, 1999 (1992).
- ¹²K. Ono, H. Ohta, and K. Eriguchi, *Thin Solid Films* **518**, 3461 (2010).
- ¹³S. A. Vitale, H. Chae, and H. H. Sawin, *J. Vac. Sci. Technol., A* **19**, 2197 (2001).
- ¹⁴J. W. Coburn, *Thin Solid Films* **64**, 371 (1979).
- ¹⁵K. Koshino, J. Matsuo, and M. Nakamura, *Jpn. J. Appl. Phys.* **32**, 3063 (1993).
- ¹⁶S. Banna *et al.*, *IEEE Trans. Plasma Sci.* **37**, 1730 (2009).
- ¹⁷P. Bodart, M. Brihoum, G. Cunge, O. Joubert, and N. Sadeghi, *J. Appl. Phys.* **110**, 113302 (2011).
- ¹⁸M. A. Lieberman and A. J. Lichtenberg, *Principles of Plasma Discharges and Materials Processing* (Wiley-Interscience, New York, 1994).
- ¹⁹J. Schulze, E. Schüngel, and U. Czarnetzki, *Appl. Phys. Lett.* **100**, 024102 (2012).
- ²⁰V. M. Donnelly and N. Layadi, *J. Vac. Sci. Technol., B* **16**, 1571 (1998).
- ²¹P. Sigmund, *Phys. Rev.* **184**, 383 (1969).
- ²²W. D. Wilson, L. G. Haggmark, and J. P. Biersack, *Phys. Rev. B* **15**, 2458 (1977).
- ²³P. C. Zalm, *J. Appl. Phys.* **54**, 2660 (1983).
- ²⁴H. F. Winters and E. Taglauer, *Phys. Rev. B* **35**, 2174 (1987).
- ²⁵C. Steinbrüchel, *Appl. Phys. Lett.* **55**, 1960 (1989).
- ²⁶M. E. Barone and D. B. Graves, *J. Appl. Phys.* **78**, 6604 (1995).
- ²⁷N. Layadi, V. M. Donnelly, J. T. C. Lee, and F. P. Klemens, *J. Vac. Sci. Technol., A* **15**, 604 (1997).
- ²⁸V. M. Donnelly and A. Kornblit, *J. Vac. Sci. Technol., A* **31**, 050825 (2013).
- ²⁹G. S. Oehrlein, J. F. Rembetski, and E. H. Payne, *J. Vac. Sci. Technol., B* **8**, 1199 (1990).
- ³⁰G. S. Oehrlein and Y. Kurogi, *Mater. Sci. Eng., R* **24**, 153 (1998).
- ³¹L. Desvoivres, L. Vallier, and O. Joubert, *J. Vac. Sci. Technol., B* **19**, 420 (2001).
- ³²J. M. Lane, K. H. A. Bogart, F. P. Klemens, and J. T. C. Lee, *J. Vac. Sci. Technol., A* **18**, 2067 (2000).
- ³³T. J. Dalton, J. C. Arnold, H. H. Sawin, S. Swan, and D. Corliss, *J. Electrochem. Soc.* **140**, 2395 (1993).
- ³⁴M. A. Vyvoda, M. Li, D. B. Graves, H. Lee, M. V. Malyshev, F. P. Klemens, J. T. C. Lee, and V. M. Donnelly, *J. Vac. Sci. Technol., B* **18**, 820 (2000).
- ³⁵K. P. Giapis and G. S. Hwang, *Thin Solid Films* **374**, 175 (2000).
- ³⁶A. P. Mahorowala and H. H. Sawin, *J. Vac. Sci. Technol., B* **20**, 1077 (2002).
- ³⁷S. Samukawa and K. Terada, *J. Vac. Sci. Technol., B* **12**, 3300 (1994).
- ³⁸S. Samukawa and T. Mieno, *Plasma Sources Sci. Technol.* **5**, 132 (1996).
- ³⁹T. H. Ahn, K. Nakamura, and H. Sugai, *Plasma Sources Sci. Technol.* **5**, 139 (1996).
- ⁴⁰G. S. Hwang and K. P. Giapis, *Jpn. J. Appl. Phys.* **37**, 2291 (1998).
- ⁴¹J.-H. Kim, C.-J. Kang, T.-H. Ahn, and J.-T. Moon, *Thin Solid Films* **345**, 124 (1999).
- ⁴²S. Samukawa, K. Noguchi, J. I. Colonell, K. H. A. Bogart, M. V. Malyshev, and V. M. Donnelly, *J. Vac. Sci. Technol., B* **18**, 834 (2000).
- ⁴³K. P. Giapis, G. S. Hwang, and O. Joubert, *Microelectron. Eng.* **61**, 835 (2002).
- ⁴⁴M. Haass, M. Darnon, and O. Joubert, *J. Appl. Phys.* **111**, 124905 (2012).
- ⁴⁵H. Hübner, *J. Electrochem. Soc.* **139**, 3302 (1992).
- ⁴⁶G. Cunge, R. L. Inglebert, O. Joubert, L. Vallier, and N. Sadeghi, *J. Vac. Sci. Technol., B* **20**, 2137 (2002).
- ⁴⁷X. Detter, R. Palla, I. Thomas-Boutherin, E. Pargon, G. Cunge, O. Joubert, and L. Vallier, *J. Vac. Sci. Technol., B* **21**, 2174 (2003).
- ⁴⁸G. Cunge, M. Kogelschatz, O. Joubert, and N. Sadeghi, *Plasma Sources Sci. Technol.* **14**, S42 (2005).